

# Variation in Reflected Beam Shape and Pointing Accuracy Over Time and Heliostat Field Position

Randy C. Brost<sup>1</sup>, Anthony Evans<sup>1</sup>, Kevin Good<sup>1</sup>, Luis Garcia Maldonado<sup>1</sup>,  
and Tristan Larkin<sup>1</sup>

<sup>1</sup> Sandia National Laboratories

**Abstract.** Heliostats are typically constructed with fixed mirror shapes, which they move to varying angles to reflect sunlight onto a receiver. While heliostat facet curvatures and canting angles are selected to maximize a chosen performance criterion, these fixed shapes inevitably cannot maintain focus throughout widely varying solar incidence angles. Further, heliostat pointing accuracy generally exhibits error due to manufacturing and installation imperfections. In this paper we present a systematic study of how reflected beam shape and pointing accuracy vary with heliostat position, time of day, and time of year. We selected nine heliostats spanning the Sandia National Laboratories National Solar Thermal Test Facility (NSTTF) heliostat field, and measured their beam shape and required pointing corrections throughout the day, for six key dates spanning a solar year. We also present ray tracing analysis to aid understanding of the observed effects. The resulting data provide insight into the nature and magnitude of heliostat focus loss at various times, and clarify the nature of the problem faced when attempting to maximize heliostat field performance, especially for high-temperature industrial applications. We conclude that fixed heliostat fields canted with an off-axis strategy will lose significant performance away from the solar noon hour to which they are tuned, and that aim point corrections can vary widely, both between independent heliostats and over time for a given heliostat. This implies that multiple measurements of each heliostat are required to determine calibration pointing corrections.

**Keywords:** Heliostat, Heliostat focus, Heliostat calibration, Heliostat canting

## 1. Introduction

Heliostat fields can simultaneously achieve very high temperature and very high power. For example, the Sandia National Solar Thermal Test Facility (NSTTF) heliostat field can achieve solar concentration ratios of 2,500 suns with a power of 5 MW<sub>th</sub>, heating samples to over 1,400°C (Figure 1). This requires each heliostat to focus a tight beam of light onto the receiver, at the proper aim point.

But heliostats with a fixed optical shape cannot remain focused throughout the day. Variation in sun position causes sunlight to arrive with widely varying incidence angles off the heliostat's nominal optical axis, causing a loss of focus. This effect has been recognized for decades [1]. The magnitude of the effect varies with heliostat location, time of day, and time of year. For heliostat fields in the northern hemisphere, a heliostat due north of the tower may see a range of sunlight incidence angles varying over roughly [−45°, +45°]. In contrast, a heliostat due west of the tower may see incidence angles varying over [0°, +90°]. Each heliostat sees different off-axis incidence conditions, which can vary greatly over time.

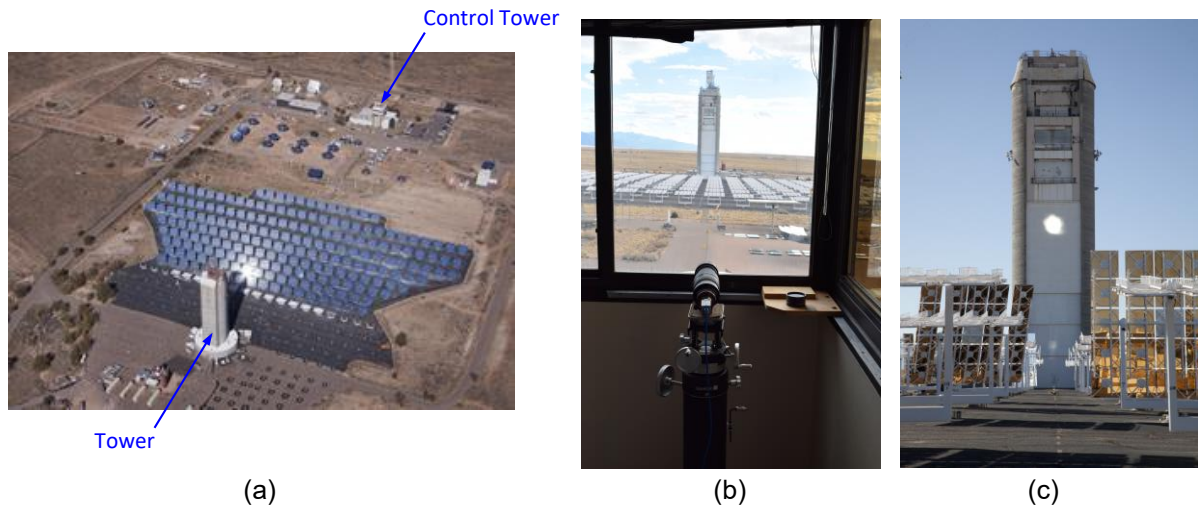


**Figure 1.** (a) Sandia NSTTF heliostat field. (b) BCS camera. (c) Reflected spot on tower.

Meanwhile, heliostat pointing errors also affect performance. Due to various causes, heliostat pointing errors are not a simple constant offset. Instead, they vary with sun position, implying that aiming corrections cannot be modeled as simple parameters. Past work to calibrate heliostat fields has recognized this and employed calibration schemes that produce complex multivariate correction functions [2], [3], [4].

This paper reports an experiment where we directly measured the variation in reflected beam shape and pointing accuracy that occurs throughout the day and year for nine key heliostats in the NSTTF heliostat field (Figure 2). The following sections will explain these experiments in detail.

## 2. Beam Shape

To obtain measures of both beam shape and pointing accuracy, we utilized the beam characterization system (BCS) [5]; see Figure 1(b). In our experiment we commanded heliostats one at a time to reflect sunlight onto the tower BCS target, and captured images of the resulting spot. Figure 1(c) shows an example. For the beam shape study, we collected images for all nine heliostats at times just after sunrise, just before sunset, solar noon, and mid-morning and mid-afternoon times roughly halfway between these times.

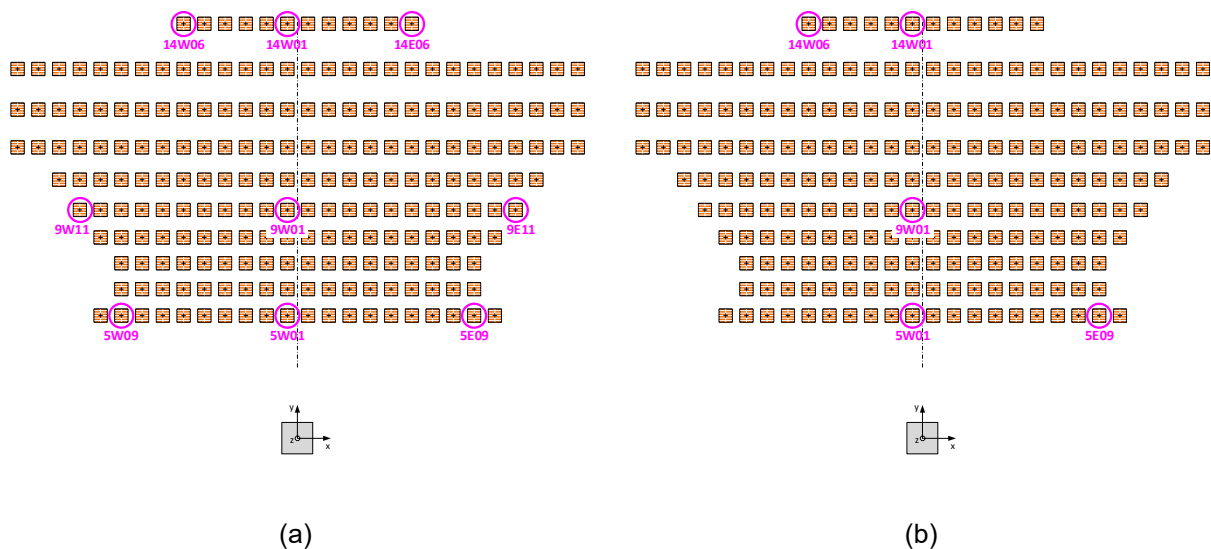


**Figure 2.** Heliostats measured (a) for beam shape, (b) for pointing accuracy.

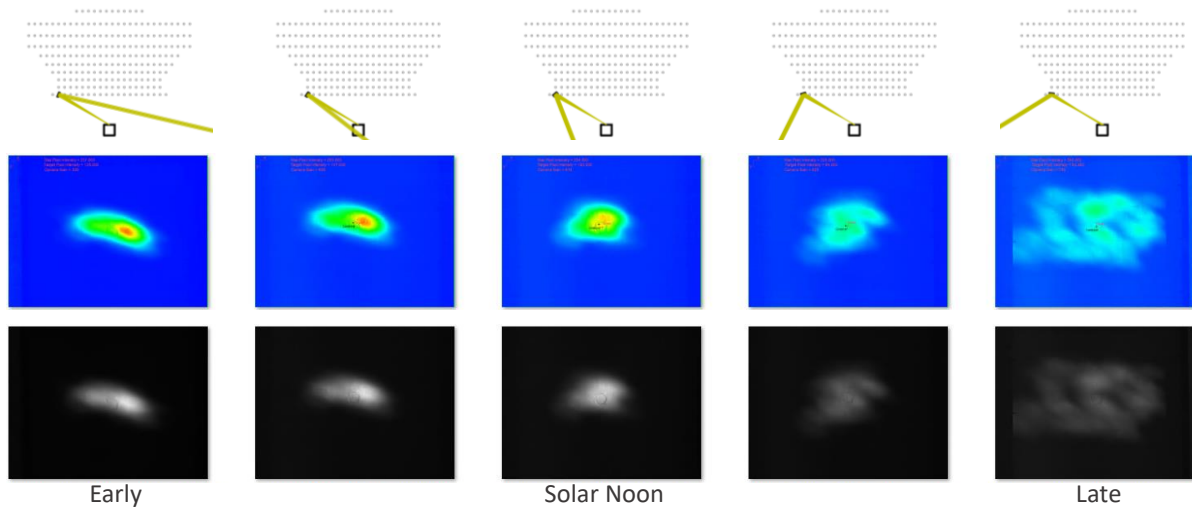


**Figure 3.** Beam shape variation throughout one day for heliostat 5W09. Left-to-right shows time from early morning, through solar noon, to late evening. Bottom row shows raw BCS images; middle row colored to highlight beam intensity. Top row ray trace shows field position and incidence angle.

Figure 3 shows the result for heliostat 5W09 on February 10, 2023. Left-to-right corresponds to morning to evening. We see a tight focus in the morning (elliptical due to the beam’s oblique angle to the target), and a highly diffuse spot late in the day.

Why? The Figure 3 ray trace images show how solar incidence angle changes from near-normal in the morning to far off-normal in the evening. The effect of varying incidence angle is illustrated in Figure 4. This simple 2-d ray tracing model treats the sun as a point source, and models a rigid heliostat canted for tight focus at  $0^\circ$  incidence (a). As incidence angle increases, the reflected beam spreads substantially (b,c). This is because a fixed heliostat shape cannot focus across multiple incidence angles.

Figure 5 shows the same-day results for all nine assessed heliostats, and Figure 6 shows the results across the solar year. Careful study of these data reveals a number of insights: These effects are common across the solar field, of lower magnitude for heliostats north of the tower than off to the side, and all heliostats perform well at solar noon. This is because NSTTF heliostats are canted with an off-axis strategy that sets best focus at solar noon on the equinox. We also note that loss of focus effects are magnified in summer; this is because for NSTTF Earth location and tower geometry, vertical off-axis incidence is higher in summer than winter.

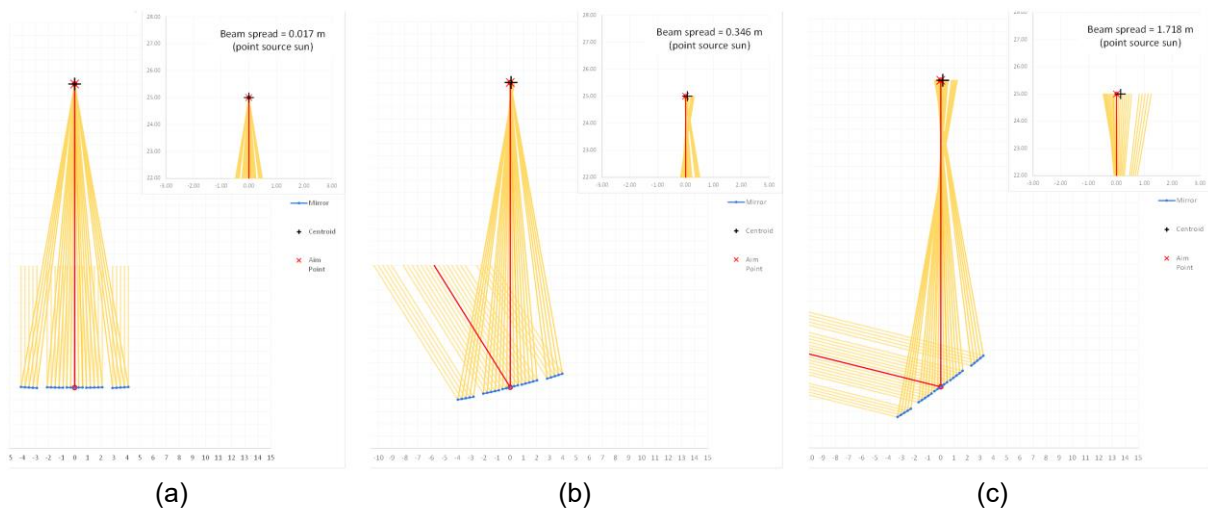


**Figure 4.** Simple 2-d ray trace showing effect of off-axis incidence. (a)  $0^\circ$ . (b)  $30^\circ$ . (c)  $75^\circ$ .

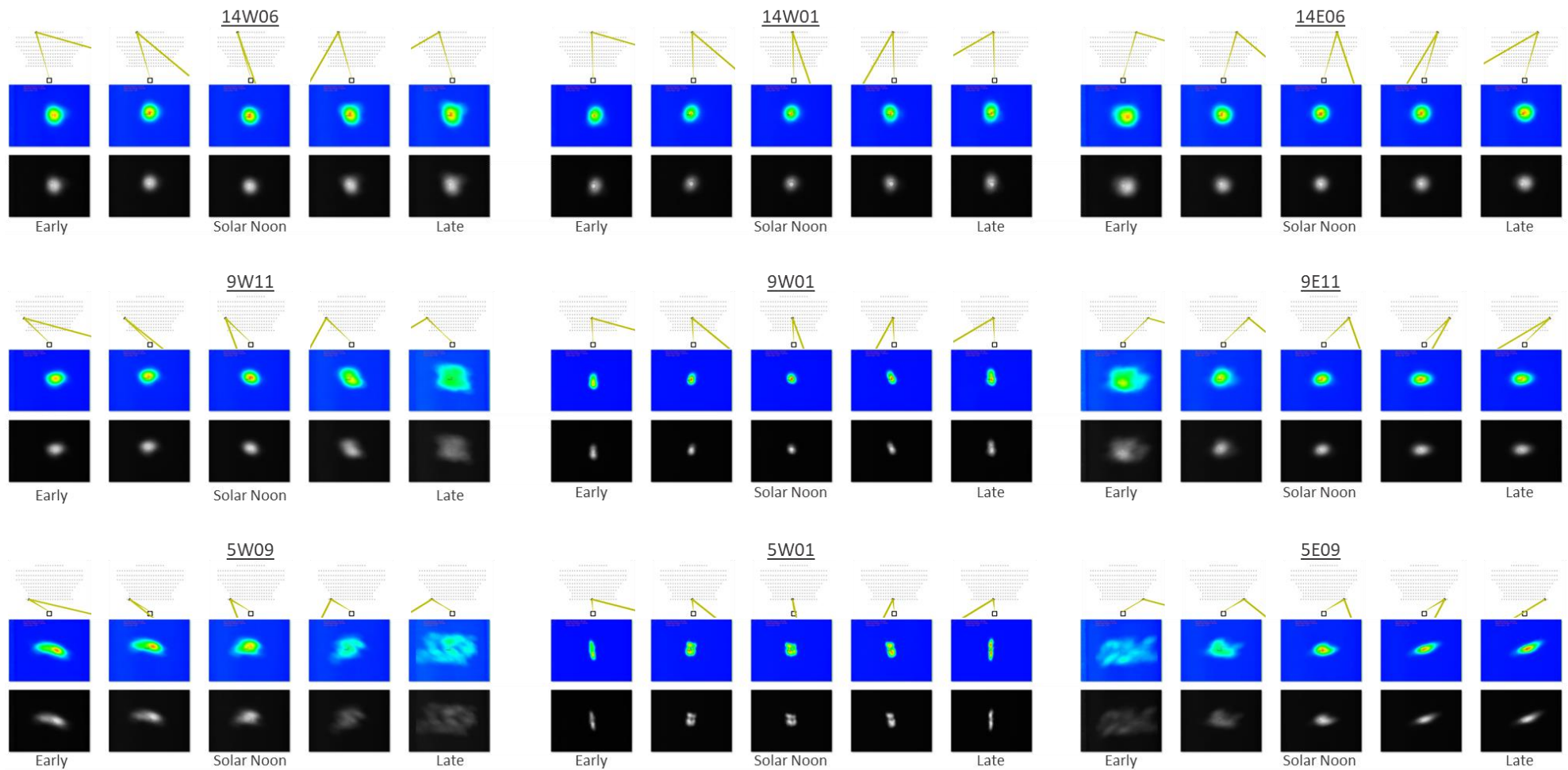


**Figure 5.** Beam shape variation for the nine measured heliostats over a single day (February 10, 2023). Each block shows beam spot from just after sunrise until just before sunset; the middle image is near solar noon. Evening-West  $\leftrightarrow$  Morning-East symmetries, and their complements, are readily apparent. Ray trace icons clarify that beam defocus is attributable to high incidence angles. All heliostats are well-focused at solar noon, consistent with off-axis canting.

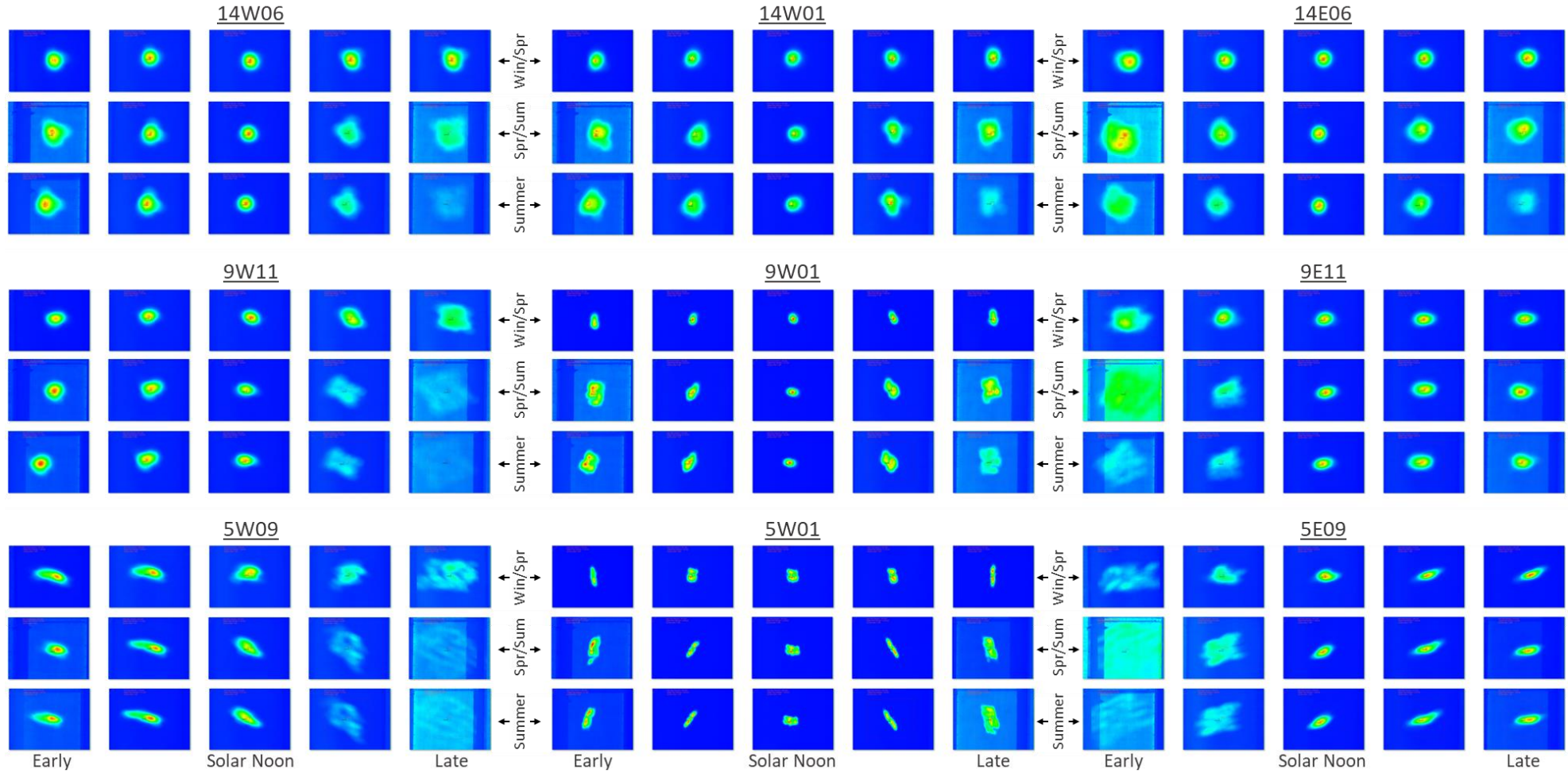


**Figure 6.** Beam shape variation for the nine measured heliostats across a year. Each block shows beam spot from just after sunrise until just before sunset; the middle image is near solar noon. Left-to-right shows time from early morning to late evening; top-to-bottom shows time from winter to summer.

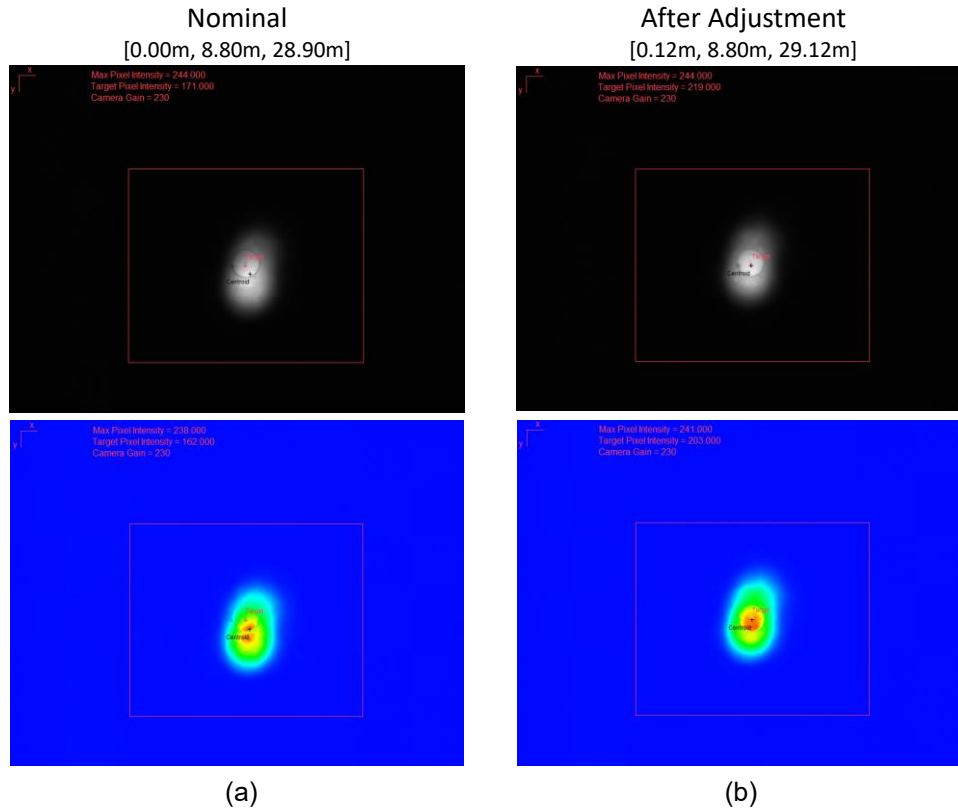


**Figure 7.** Measuring correction required to achieve accurate beam pointing.  
 (a) Heliostat commanded to point at target. (b) After correcting commanded aim point.  
 Top: Raw BCS images, with BCS control interface annotations.  
 Bottom: Colored to improve perception of variation in beam intensity.

### 3. Pointing Accuracy

We also used the BCS system to measure heliostat pointing accuracy. Our measurement process is shown in Figure 7. We first directed the heliostat to aim its reflected beam onto the BCS target [0.0m, 8.8m, 28.9m] and captured an image (Figure 7(a)). The BCS control software simultaneously displays the target point (red “+”) and the current spot centroid (black “+”). Discrepancies between these indicate pointing error. We then adjusted the aim point until the red “+” and black “+” coincide. The correction is then the difference between the two commanded points. In Figure 7, [0.12m, 8.8m, 29.12m] – [0.00m, 8.8m, 28.90m] ⇒ correction = [+0.12m, 0.0m, +1.22m]. We repeated this process throughout the day. To increase temporal resolution, we reduced the heliostats to those shown in Figure 2(b).

The results are summarized in Figure 8. The left column reports X component of the correction and the right column reports Z the component. Each row corresponds to a different measured heliostat. All times are normalized to hours relative to solar noon. Colors indicate sample date, transitioning from cold blue for winter to hot red for summer.

Our manual measurement process had significant uncertainty, and particular points – such as 5E09 in the early morning – have higher uncertainty due a highly diffuse spot. Nonetheless, we estimate the uncertainty to be much smaller than the systematic trends seen in heliostats such as 5E09, 14W01, and 14W06. We can observe significant trends both within a day and across the year.

The variability in these data imply that heliostat calibration will require multiple correction observations for each heliostat, sampled across its working envelope.

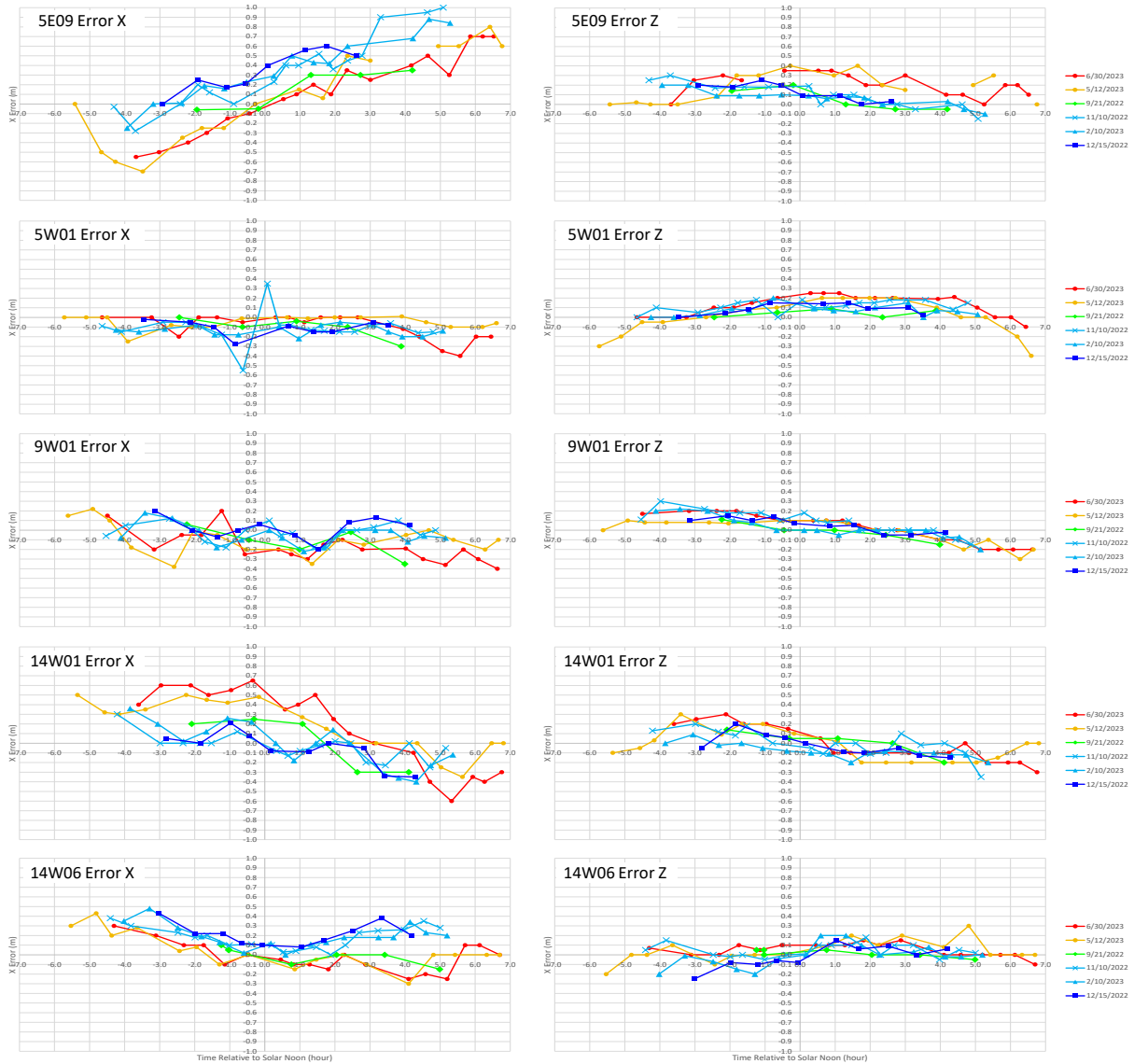


**Figure 8.** Measured pointing corrections. Left: Correction in X direction. Right: Correction in Z direction. Horizontal axis shows time relative to solar noon ( $t = 0$ ). Vertical axis shows magnitude of correction in meters. Curve colors vary from winter (blue) to summer (red).

## 4. Discussion

We report direct measurement of the variation in beam shape and pointing accuracy for real heliostats in an operational heliostat field. Variations in both were quite substantial – changes in beam shape were sometimes severe enough that detecting the spot on the tower became difficult. Pointing errors up to 0.4 m were observed, which could reduce energy capture for a (1.6m × 1.6m) square receiver by approximately 25%.

We note that Figure 4 shows an on-axis canting example for simplicity. More sophisticated off-axis canting and other strategies [6], [7] can modify but not eliminate this effect. (For example, NSTTF is canted to an off-axis strategy, yet the results in Figures 5 and 6 remain.) The inability of fixed-shape heliostats to maintain focus throughout the day has motivated the pursuit of variable focus heliostats [8], [9].

## Data availability statement

The data reported in this paper is publicly available, To access the data, send inquiries to OpenCSP@sandia.gov.

## Author contributions

Randy Brost contributed experiment design, data collection, data curation, data processing, analysis, 2-d ray tracing, funding acquisition, project administration, and writing. Anthony Evans, Kevin Good, and Luis Garcia Maldonado contributed detailed data collection. Tristan Larkin contributed ray tracing and writing.

## Competing interests

The authors declare that they have no competing interests.

## Acknowledgement

We thank Benson Tso, Robert Crandell, and Roger Buck for heliostat field support and troubleshooting. Sandia National Laboratories is a multi-mission laboratory managed and operated by National Technology & Engineering Solutions of Sandia, LLC, a wholly owned subsidiary of Honeywell International Inc., for the U.S. Department of Energy's National Nuclear Security Administration under contract DE-NA0003525. This written work is authored by an employee of NTESS. The employee, not NTESS, owns the right, title and interest in and to the written work and is responsible for its contents. Any subjective views or opinions that might be expressed in the written work do not necessarily represent the views of the U.S. Government. The publisher acknowledges that the U.S. Government retains a non-exclusive, paid-up, irrevocable, world-wide license to publish or reproduce the published form of this written work or allow others to do so, for U.S. Government purposes. The DOE will provide public access to results of federally sponsored research in accordance with the DOE Public Access Plan.

## References

1. A. Rabl. *Active Solar Collectors and Their Applications*. Oxford University Press, ISBN 978-0195035469, 1985.
2. S. Khalsa, et al. An Automated Method to Correct Heliostat Tracking Errors. *SolarPaces 2011*.
3. M. Ayres, et al. Heliostat Aiming Corrections with Bad Data Detection. *SolarPaces 2019*.
4. J. C. Sattler, et al. Review of heliostat calibration and tracking control methods. *Solar Energy* **207**, 2020.
5. J. Strachan. Revisiting the BCS, a Measurement System for Characterizing the Optics of Solar Collectors. Sandia Report SAND92-2789C, 1992.
6. R. Buck and E. Tuefel. Comparison and Optimization of Heliostat Canting Methods. *Journal of Solar Energy Engineering* **131**, February 2009.
7. W. Landman and P. Gauche. Influence of canting mechanism and facet profile on heliostat field performance. *Energy Procedia* **49**, pp. 126-135, 2014.
8. A. Lehmann and P. Allenspach. Toroidal Heliostat. United State Patent 9,454,001, September 2016.
9. R. Angel, et al. Actively Shaped Focusing Heliostat. *SolarPACES 2020*.